# Highway-Bridge Impact Problems

T. P. TUNG, Research Assistant Professor of Civil Engineering, University of Illinois
L. E. GOODMAN, formerly Research Associate Professor of Civil Engineering, University of Illinois and now Professor of Mechanics and Materials, University of Minnesota
T. Y. CHEN, Research Assistant Professor of Civil Engineering, and
N. M. NEWMARK, Research Professor of Structural Engineering, University of Illinois

This paper is a review of analytical and experimental research at the University of Illinois on the highway bridge impact problem. Examples of analytical results obtained on a high speed digital computer are presented for a series of problems of increasing practical importance including: (1) a single rigid mass moving at constant velocity over a flexible beam; (2) a single sprung mass moving at constant velocity over a flexible beam, starting with zero initial deflection and zero initial bouncing velocity; and (3) a sprung mass oscillating with some definite amplitude of oscillation, moving at constant velocity over a flexible beam, arranged in phase of the bouncing motion so that the mass produces approximately the worst possible condition in the beam. Consideration is given to other factors and a brief discussion is made of their importance.

Comparisons are made of the results of the analyses with other theoretical results and with results of carefully made experiments of the effect of rolling sprung and unsprung masses on a small elastic beam. The results of the comparisons indicate that the data obtained from the analysis are dependable and accurate.

The general problem of impact on highway bridges is discussed with a view toward design applications of the results of the research program, and the planning of future studies in the program.

## Purpose and Scope of the Study

● IN the structural design of highway bridges, the live load static stresses are increased by applying an impact factor so that sufficient provision is made for the stresses produced by the dynamic response of the bridge to moving loads. A program of research of this subject was begun in July 1950, as a cooperative project between the Engineering Experiment Station, University of Illinois, the Illinois Division of Highways, and the Department of Commerce, Bureau of Public Roads. The primary purpose of the project was to make investigations and tests to determine the dynamic behavior of highway bridges, to assess the relative importance of the various factors that influence the dynamic stresses in highway bridges, and to obtain information which will be useful as a guide in the proper selection of impact factors in highway bridge design.

The problem at hand is a complicated one because of the widely varying conditions under which highway bridges function and because of the great variety of factors which affect, in varying degrees, their dynamic behavior. An idea of the complicated nature of the dynamic behavior of a highway bridge when a vehicle crosses its span may be obtained by considering first an over-simplification of the actual problem: the effect of a constant force moving across a straight, smooth beam. If the force moves very slowly, the beam merely deflects, and its deflection curve is, for all practical purposes, the same as the static deflection curve. However, if the force does not move slowly, deflections as well as vibrations are set up in the beam. The total deflection in the beam at any instant during the passage of the force is then a combination of the static deflection and the natural or free vibration of the beam. Hence, the deflection of the beam caused by a moving constant force is a function of the span, mass, stiffness, and damping characteristics of the beam as well as the magnitude and speed of the force.

Now, in the actual bridge-vehicle system, matters are far more complex. First

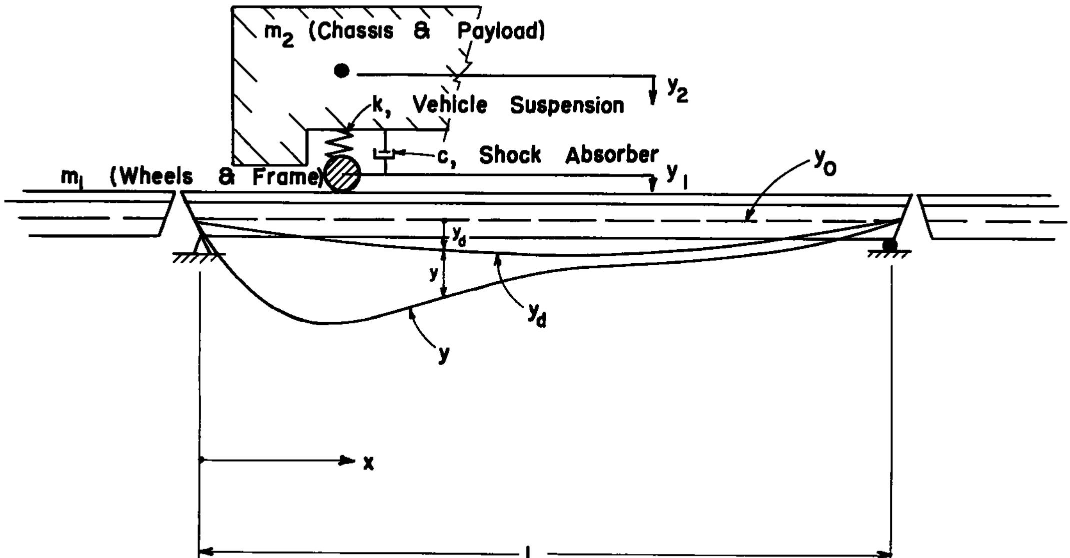


Figure 1. Schematic diagram showing vehicle-bridge system.

of all, the body of a vehicle is usually supported along its sides by pairs of springs, mounted near the ends of each of two or more axles. When the vehicle is in motion, the body oscillates on the springs, either in phase or out of phase with the motion of the vehicle or of the bridge. Thus, the vehicle with its springs and tires is in itself a complex mass-spring vibratory system, and the force it exerts on the bridge is by no means a single constant force as considered in the above simplification. The load applied by the vehicle on the bridge is divided between the axles, and the force on each axle is a function of the speed, mass, and springing characteristics of the vehicle, the elasticity of the tires, and above all, because of the interaction between the bridge and the vehicle, the motion of the bridge. This condition is further complicated by the fact that the bridge actually is not a single, straight, and smooth beam, but a not perfectly smooth surface in motion, with the probable presence of bumps, low spots, or waviness in the road surface, or of curvature in alignment. As a result, in adverse conditions the vehicle may even sway laterally, simultaneously with its vertical vibratory motion, thereby producing roll effects on the stresses in the bridge in addition to the speed effects.

An analysis of the dynamic behavior of a highway bridge system taking into account all of the factors just described would involve extreme complexity and difficulty. In a study of this nature, assumptions and simplifying approximations must be made to render a solution of the problem feasible. The investigation reported herein therefore has been planned to cover three idealized groups of problems, mainly dealing with simply supported slab type or slab-and-beam type of highway bridges, which are listed below in the order of increasing practical importance:

(1) A single rigid mass moving at constant velocity over a flexible beam.

(2) A single sprung mass moving at constant velocity over a flexible beam, starting with zero initial deflection and zero initial bouncing velocity.

(3) A sprung mass moving at constant velocity over a flexible beam, and initially oscillating with some definite amplitude such that the mass produces approximately the worst possible conditions in the beam.

In the above three groups of problems, the investigations and the conclusions drawn therefrom concern specifically the speed effect of a vehicle only. The roll effect due to lateral sway of the vehicle has not been considered.

## General Procedure

Throughout the work, a combination of analytical and experimental study has been used. To a large extent, it has been the practice first to derive the analytical solutions and then, by testing structures of proportions selected for their practical importance, to test the validity of the assumptions made in the analysis and hence to study the applicability of the analytical solutions. The analytical results were obtained with the aid of the ILLIAC, a high speed electronic digital computer, in a manner which will be described briefly herein. The experimental program has been confined to laboratory model tests conducted on specially designed and carefully controlled testing equipment.

## Assumptions

The following assumptions are made in the investigation: (1) Simply supported slab or slab-and-beam bridges behave as simply supported flexible beams. (2) The structures are considered to be linearly elastic. (3) A vehicle is considered to consist of two parts: (a) the sprung part, which is the chasis and payload; and (b) the unsprung part, which consists of the wheels and frame. A linear spring is inserted between the two parts to provide for the effect of vehicle suspension. (4) The effect of flexibility of tires is neglected. (5) The speed of a vehicle is constant during its passage over the bridge. (6) Only one single axle-load is specifically considered. (The words "vehicle weight" and "axle load" have been used interchangeably where it is believed no confusion would result.) Simultaneous loading on more than one lane is not considered. (7) The wheels of the vehicle are assumed to be in contact with the bridge throughout the passage of the vehicle over the bridge. There are no obstacles on the road surface of the bridge. (8) Prior to the entrance of a vehicle, the bridge is not vibrating; that is, it is initially stationary. (9) Effects of camber, roadway unevenness, damping of the bridge, and damping of the vehicle oscillation by shock absorbers are considered in the derivation of the general equations, but are neglected in the present computations of numerical results.

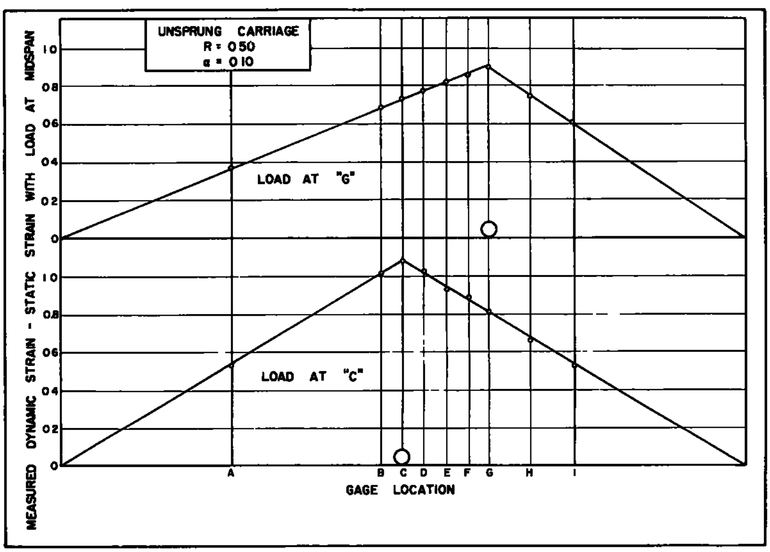


Figure 2. Instantaneous stress distribution.

# ANALYTICAL INVESTIGATION

## General Concepts

When a vehicle enters a highway bridge span, the part of the bridge under the load acquires a downward deflection. Later on, the bridge, being elastic, tends to rebound; and during the interval of passage the bridge and the vehicle, which is also a flexible structure, interact on each other in a complex way. To simplify matters somewhat, it is convenient to consider an idealized vehicle-bridge system as shown schematically in Figure 1.

In Figure 1, $y_o(x)$ represents the unstressed shape of the neutral axis of the cross-section of a slab or slab-and-beam bridge; $y_d(x)$ represents the dead load deviation from $y_o(x)$; and $y(x, t)$ represents a further deflection of the bridge after a moving load has entered the span. Next consider the axle load applied to the bridge. The part of the vehicle consisting of the wheels and frame and having mass $m_1$, undergoes a deflection $y_1(t)$; and the part of the vehicle consisting of the chassis and payload and having mass $m_2$, undergoes a deflection $y_2(t)$, both of which are measured from their position of static equilibrium. A spring having a spring constant k, and a viscous damping element c, inserted between the two masses $m_1$ and $m_2$, account for the effects of vehicle suspension and shock absorber, respectively.

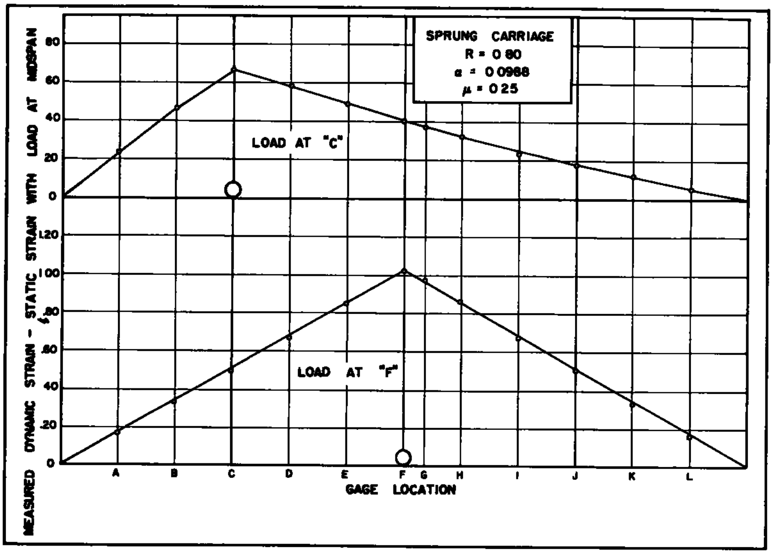


Figure 3. Instantaneous stress distribution.

## Equations of Motion

By considering the energies of the vehicle-bridge system shown in Figure 1, the equations of motion may be derived in the following manner.

Corresponding to the initial dead load configuration $y_d(x)$, the strain energy stored in the bridge may be expressed as

$$U_d = \tfrac{1}{2} \int_0^L EI\,(y''_d)^2\,dx, \tag{1}$$

in which the superscript dashes denote differentiation with respect to x. After a moving load enters the bridge, the bridge undergoes a further deflection y(t), making the total strain energy stored in the bridge become

$$U_b = U_d + \int_0^L mg\,y\,dx + \tfrac{1}{2} \int_0^L EI\,(y_{xx})^2\,dx, \tag{2}$$

in which m is the mass of the bridge per unit of length, and the subscript x indicates partial differentiation with respect to x, repeated as many times as the subscript is repeated.

The total strain energy stored in the vehicle, for each axle, is given by

$$U_v = \tfrac{1}{2}\,k\,d^2 + m_2 g\,(y_2 - y_1) + \tfrac{1}{2}\,k\,(y_2 - y_1)^2\,, \tag{3}$$

in which d is the initial compression in the spring in the static equilibrium state, from which $y_2$ is measured.

The total potential energy of the vehicle-bridge system may then be written as

$$U = U_b + U_v - \tfrac{1}{2} \int_0^L mg\, y_d\, dx - \int_0^L mg\, y\, dx$$

$$- m_2 g \left(y_2 + \frac{d}{2}\right) - m_1 g\, y_1 \quad ,$$

which, in view of Equations (2) and (3), reduces to

$$U = \tfrac{1}{2} \int_0^L EI\, (y_{xx})^2\, dx - (m_1 + m_2)\, g\, y_1 + \tfrac{1}{2} k\, (y_2 - y_1)^2$$

$$+ \left[ U_d + \tfrac{1}{2} k\, d^2 - m_2 g\, \frac{d}{2} - \tfrac{1}{2} \int_0^L mg\, y_d\, dx \right] . \qquad (4)$$

In Equation (4) the terms in square brackets are constants that reflect the choice of the initial energy level at that corresponding to a "true" zero, and may therefore be disregarded, for simplicity's sake, in subsequent derivation without affecting the final form of the equations of motion.

The kinetic energy of the whole system is given by

$$T = \tfrac{1}{2} \int_0^L m\, (y_t)^2\, dx + \tfrac{1}{2} m_1\, \dot{y}_1^2 + \tfrac{1}{2} m_2\, \dot{y}_2^2 \quad , \qquad (5)$$

in which the superscript dots denote total derivatives with respect to time t, and $y_t = \frac{\partial y}{\partial t}$ .

As the bridge and the vehicle are not perfectly elastic, account must also be taken of the rate at which work is done by the damping forces. Assuming that damping forces are proportional to velocities, we may express the dissipation function D by

$$D = \tfrac{1}{2} c\, (\dot{y}_2 - \dot{y}_1)^2 + \tfrac{1}{2} c' \int_0^L \dot{y}^2\, dx \quad , \qquad (6)$$

in which c and c' are the damping constants of the vehicle shock absorbers and the bridge respectively.

So far, the vertical motion of the wheel denoted by $y_1$ (t), has been treated as though it were independent of the motion of the bridge. By assuming that the wheels are in contact with the bridge at all times, the relation between the motions of the wheel and the bridge may be expressed by

$$y_1(t) = y_o(vt) + y_d(vt) + y(vt,\ t) \quad , \qquad (7)$$

in which v is the speed of the vehicle.

By the use of Equation (7), $y_1$ may now be eliminated from Equations (4), (5), and (6), and the expressions for U, T, and D contain as unknowns only the quantities $y_2(t)$ and y(x, t). A conventional approach would then consist in expanding y(x, t) in a series of functions which are orthogonal and complete, and which satisfy the conditions at the ends of the span, i.e., for simple supports, $y(x,t) = \sum_{n=1}^{\infty} q_n(t) \sin \frac{n\pi x}{L}$ . The integrals with respect to x could then all be written out, and the resulting expressions substituted into Lagranges' equations of motion:

$$\frac{d}{dt}\left(\frac{\partial T}{\partial \dot{q}_n}\right) - \frac{\partial T}{\partial q_n} + \frac{\partial U}{\partial q_n} + \frac{\partial D}{\partial \dot{q}_n} = 0 \quad . \qquad (8)$$

If the resulting equations are linear, and on account of the orthogonality of the characteristic functions, only one of the unknown $q_n$'s will appear in any equation. Under these circumstances, solution for $q_n$, and hence for y(x, t), would be relatively simple.

Unfortunately, however, the use of this conventional approach in the present case would only result in an infinite number of differential equations of motion, each containing an infinite number of dependent variables. To circumvent this difficulty presented by the nonlinearity of the equations of motion, several attempts to solve the problem have been made in the past; notably by Inglis (1) and by Timoshenko (2). The former procedure consists in neglecting the higher modes of oscillation, thereby introducing rather serious errors; the latter procedure consists in assuming that the effect of a constant mass traversing a beam is the same as the effect of a constant force traversing the beam. Both of these procedures are considered undesirable for the purpose of the present study.

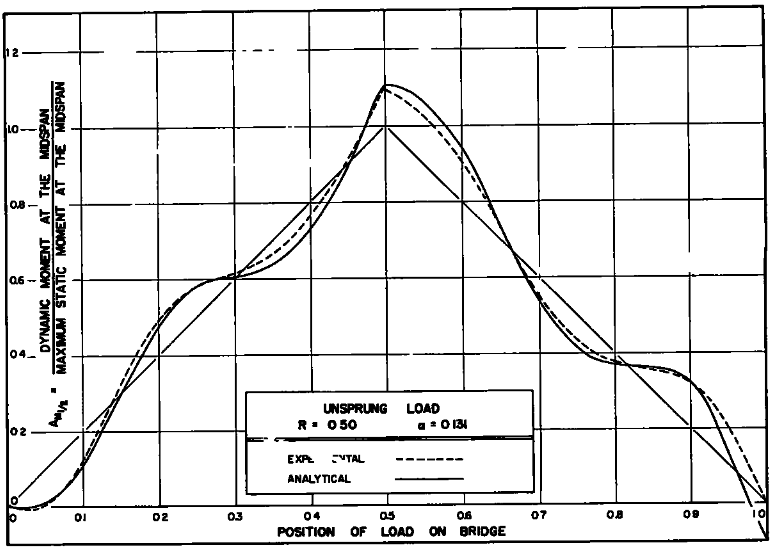


Figure 4. Moment at the midspan.

Since this difficulty existing in the equations of motion mainly arises from the nonlinearity of the vehicle-bridge interaction, which in turn is a result of the fundamental physical properties of the system, it was thought and hoped, at an early stage of this investigation, that some experimental observation might be able to show a way to arrive at some basis for a more rational and simplified analysis. A series of laboratory experiments were therefore instituted to search for general characteristics of the dynamic behavior of the vehicle-bridge system which might serve as a guide to a simplified analysis. These experiments have been described in detail in a thesis by Boehning (3). Briefly, they consisted in causing sprung and unsprung loads to traverse a 6-ft. simple span test beam at constant velocity while oscillograph records of load position, deflection, and strain as functions of time were taken at stations along the span. The data were analyzed in various ways, and it was found that graphs of the instantaneous bending moment distribution along the span indicated a way to a simplification of the equations of motion.

In Figures 2 and 3 are shown two such instantaneous stress distribution diagrams, which are typical of the many drawn up from test data covering wide ranges of parameter values defining the physical properties of the vehicle-bridge system. It was found that all of the instantaneous stress distribution curves have the simple triangular form such as indicated in Figures 2 and 3. This triangular form of instantaneous stress distribution states in effect that, for the proportions of the highway bridges considered in this study, the dynamic stress distribution at any instant is the same as the static stress distribution except that it is everywhere multiplied by a factor. The factor in question varies in magnitude with the weight and velocity of the load and with its position on the bridge (hence with time), but it is the same, at any instant, throughout the bridge.

Based on this experimental finding, then, a simplifying approximation was introduced at this stage of the analytical study. The approximation consists in assuming that the dynamic deflection y (x, t) caused by live load plus impact of a bridge of uniform cross section is given by the product of $f(x,t)$, which is the deflection at any point of a simple beam under a concentrated force acting at the point $x = vt$, multiplied by $q(t)$, a factor which varies with time, but which is independent of x. That is,

$$\left.\begin{aligned} &y(x,t) = q(t)\ f(s,t) \quad , \\ \text{in which}\quad &f(x,t) = \sum_{n=1}^{\infty} \frac{1}{n^4} \sin\frac{n\pi x}{L} \sin\frac{n\pi vt}{L} \ . \end{aligned}\right\} \qquad (9)$$

On substituting Equation (9) into the expressions for $y_1(t)$, U, T, and D, we obtain

$$\left.\begin{aligned} y_1(t) &= q(t)f(vt,\ t) + y_d(vt) + y_o(vt) \text{ (under load);} \\ U &= \tfrac{1}{2} EI q^2 \int_0^L f_{xx}^{\ 2}\,dx + \tfrac{1}{2} k (y_2 - y_1)^2 - (m_1 + m_2) g y_1; \\ T &= \tfrac{1}{2} m \left[\dot q^2 \int_0^L f^2\,dx + 2 q \dot q \int_0^L f f_t\,dx + q^2 \int_0^L f_t^{\ 2}\,dx\right] \\ &\quad + \tfrac{1}{2} m_1 \dot y_1^2 + \tfrac{1}{2} m_2 \dot y_2^2 ; \\ D &= \tfrac{1}{2} c' \left[\dot q^2 \int_0^L f^2\,dx + 2 q \dot q \int_0^L f f_t\,dx + q^2 \int_0^L f_t^{\ 2}\,dx\right] \\ &\quad + \tfrac{1}{2} c (\dot y_2 - \dot y_1)^2 \ . \end{aligned}\right\} \qquad (10)$$

in which f denotes $f(x,\ t)$ and the subscript, t, denotes partial differentiation with respect to t.

The generalized coordinates, $q_n$, of Lagranges' Equation (8) are not reduced to two: q, and $y_2$. These two quantities determine the configuration of the vehicle-bridge system. There are then only two equations of motion, and these are found by performing the operations indicated in Equation (8) on the expressions in (10). The resulting equations are

$$\left.\begin{aligned} &m_2 \ddot y_2 + c (\dot y_2 - \dot y_1) + k (y_2 - y_1) = 0 ; \\ &m \int_0^L f (\ddot q f + 2 \dot q f_t + q f_{tt})\,dx + q\,EI \int_0^L f_{xx}^{\ 2}\,dx \\ &\quad + c' \int_0^L f (\dot q f + q f_t)\,dx \\ &\quad - f(vt,t) \left[m_1(g - \ddot y_1) + m_2 g + k(y_2 - y_1) + c(\dot y_2 - \dot y_1)\right] \\ &= 0. \end{aligned}\right\} \qquad (11)$$

The integrals in Equation (11) can all be written out from Equation (9) in the form of infinite series. These series converge very rapidly, and by taking the first term in each of these series, the very small errors involved are more than compensated for by the convenience and rapidity gained in the numerical computations. If this is done, the equations of motion for the vehicle-bridge system become

$$\left.\begin{aligned} &m_2 \ddot y_2 + c (\dot y_2 - \dot y_1) + k (y_2 - y_1) = 0; \\ &\tfrac{1}{2} m L \Big[\ddot q \sin^2 (\pi vt/L) + 2 (\pi v/L) \dot q \sin (\pi vt/L) \cos (\pi vt/L) \\ &\quad - q (\pi v/L)^2 \sin^2 (\pi vt/L)\Big] \\ &\quad + \tfrac{1}{2} EI\,L (\pi/L)^4 q \sin^2 (\pi vt/L) \\ &\quad + \tfrac{1}{2} c' L \left[\dot q \sin^2 (\pi vt/L) + q (\pi v/L) \sin (\pi vt/L) \cos (\pi vt/L)\right] \\ &= 0. \quad - \sin^2 (\pi vt/L) \left[m_1(g - \ddot y_1) + m_2 g + k (y_2 - y_1) + c (\dot y_2 - \dot y_1)\right] \end{aligned}\right\} \qquad (12)$$

Equations of motion essentially the same as Equation (12) were first derived by Hillerborg (4). However, he did not consider the unsprung part of the load, $m_1$, or the effects of camber and roadway unevenness as embodied in $y_d$ and $y_0$.

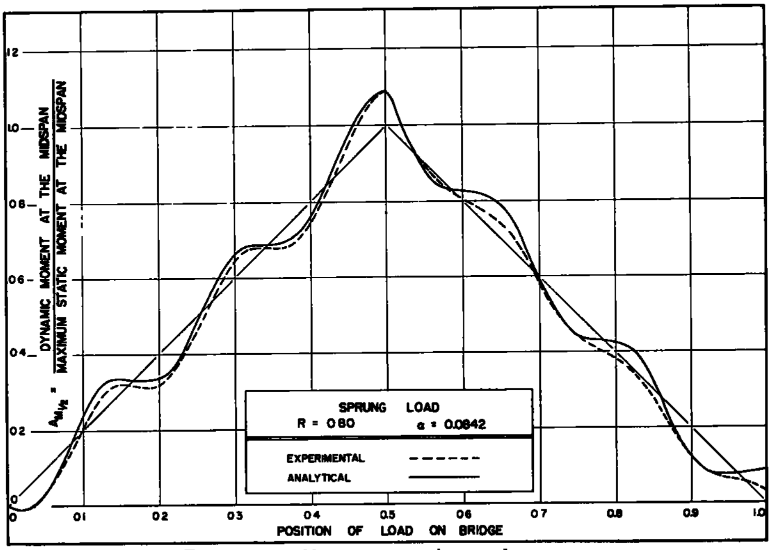


Figure 5. Moment at the midspan.

## Physical Parameters Considered

To facilitate numerical computations, it is desirable that the two equations of motion derived in the previous section be put in dimensionless forms. This step also reveals the basic physical parameters upon which the dynamic behavior of the vehicle-bridge system depends. The time variable, t, may be replaced by $\tau = vt/L$, which is a quantity proportional to t, and represents the fraction of the span traversed by the vehicle at any time. The parameters whose values directly influence numerical calculations are listed below. In the following list, as well as in subsequent calculations, the effects of damping and of camber and roadway unevenness are not considered.

Weight Parameters:

$$R_1 = \frac{\text{Wt. of unsprung part of vehicle}}{\text{Wt. of bridge}} = \frac{m_1}{mL}$$

$$R_2 = \frac{\text{Wt. of sprung part of vehicle}}{\text{Wt. of bridge}} = \frac{m_2}{mL}$$

$$R = \frac{\text{Wt. of vehicle}}{\text{Wt. of bridge}} = \frac{m_1 + m_2}{mL} = R_1 + R_2$$

Stiffness Parameter

$$\mu = \frac{\text{Fundamental period of bridge}}{\text{Fundamental period of vehicle}} = \frac{T}{T_s}$$

Speed Parameter

$$\alpha = \frac{\text{One-half the fundamental period of bridge}}{\text{Time required for the vehicle to cross the span}} = \frac{vT}{2L}$$

## Solution of Equations by Digital Computer

The equations of motion in their dimensionless forms were then solved by a numerical method of step-by-step integration, with the aid of the ILLIAC, the University of Illinois high speed electronic digital computer. The time during which a load moved from one end of the span to the other was divided into a large number of equal time

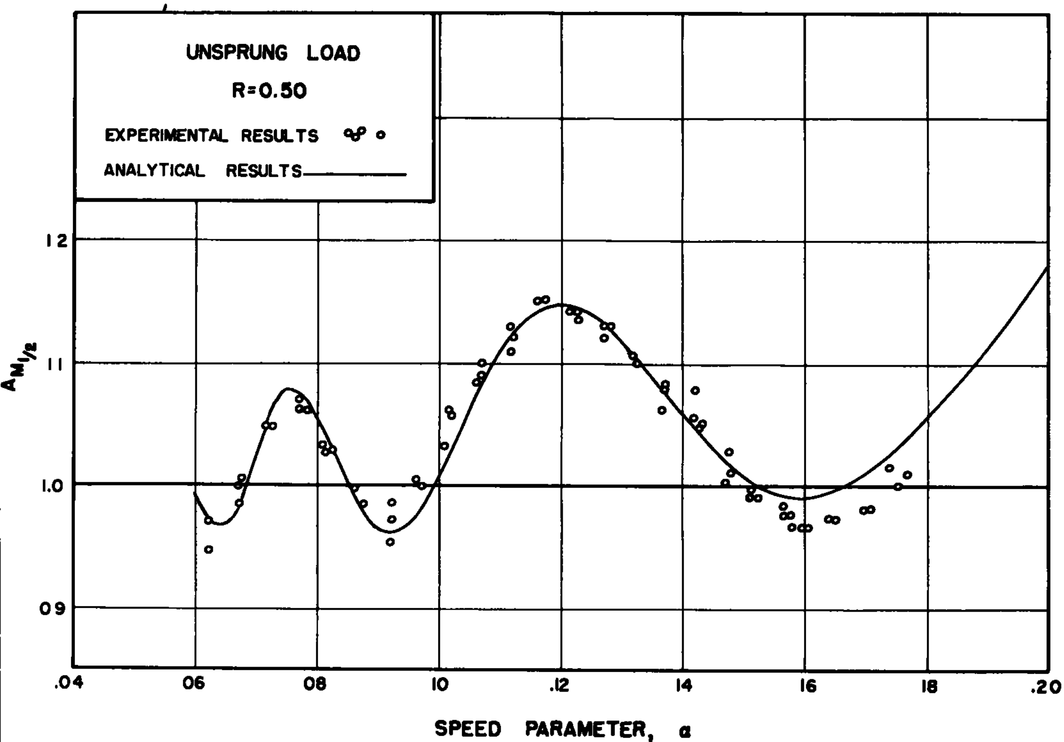


Figure 6. Amplification factor for bending moment at the second quarter point.

intervals, $\Delta\tau$. During each interval the solution was carried out on a trial and error basis. A trial value for the acceleration at the end of the time interval was assumed; the velocity and the displacement at the end of the time interval were then computed on the assumption that the variation in acceleration could be considered linear during the short time interval. The relationships used were

$$\dot{y}_n = \dot{y}_{n-1} + \tfrac{1}{2}\Delta\tau\,(\ddot{y}_n + \ddot{y}_{n-1}) \ ,$$

$$y_n = y_{n-1} + \Delta\tau\,\dot{y}_{n-1} + \frac{1}{6}\,\overline{\Delta\tau}^{\,2}\,(\ddot{y}_n + 2\,\ddot{y}_{n-1})$$

The derived acceleration was then obtained by substituting $y_n$ and $\dot{y}_n$ into the equations of motion. If the derived acceleration did not agree with the assumed value, another trial was made using the derived value as the initial assumed value. The procedure was repeated until derived and assumed values agreed within a desired degree of accuracy.

In using a step-by-step integration procedure, the length of the time interval, $\Delta\tau$, should be chosen so as to satisfy stability and convergence requirements. In the present analysis, a value of $\Delta\tau$ equal to $1/300$ of the time required for the load to cross the span was found to be satisfactory. As it was not necessary to know the bending moments and deflections at each of the 300 steps, the code for solution of the equations by the computer was so arranged that the amplifaction factors for bending moment and deflection at every sixth interval was computed.

## Test of Validity of Theory

In order to test the validity of the theory, the equations of motion were solved and the predictions were compared with test results obtained on a carefully calibrated model structure. A typical comparison is shown in Figure 4 for an unsprung load crossing a beam, and in Figure 5 for a sprung load with initially zero displacement and bouncing velocity. Referring to Figures 4 and 5, the dotted curves are oscillographic strain records re-drawn to a larger vertical scale and with ordinates converted to amplification factors for dynamic moment at mid-span of the bridge for different load positions on the span. The solid curves are corresponding analytical solutions obtained with the use of the digital computer.

Figures 4 and 5 are typical of the large number of diagrams plotted for the several series of tests conducted during the course of this investigation. The agreement between theory and experiment seems to be satisfactory in all of these comparisons.

## Results of Analysis

In view of the confidence in the theory gained from comparisons of analytical predictions and observed test results a systematic computation of the dynamic stresses produced in highway bridges of the slab and girder type has been carried out.

Unsprung Mass, and Sprung Mass with Zero Initial Displacement and Bouncing Velocity. A large number of vehicle-bridge systems were analyzed for the two cases having physical characteristics defined by parameter values that lie within the following ranges:

Weight parameter: $R = 0.20$ to $0.60$
Stiffness parameter: $\mu = 0.20$ to $0.50$
Speed parameter: $\alpha = 0.60$ to $0.20$

For the sprung case, a value of 7 was used for the ratio $R_2/R_1$, since information gathered regarding various makes and sizes of trucks indicated that this ratio ranges between 7 and 8 with values near 7.

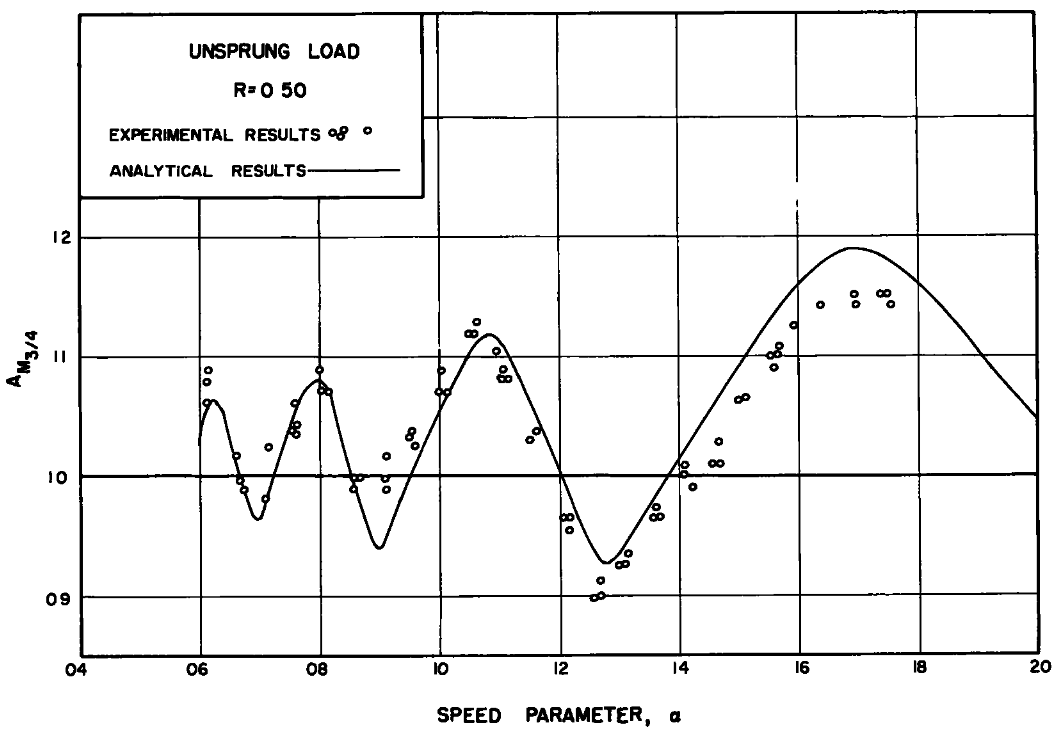


Figure 7. Amplification factor for bending moment at the third quarter point.

For each of the vehicle-bridge systems considered four quantities were determined:

$A_{M_{1/2}}$ = Amplification factor for maximum dynamic moment at mid-span based on maximum static moment at mid-span;

$A_{M\,3/4}$ = Amplification factor for maximum dynamic moment at $3/4$ point based on maximum static moment at mid-span;

$A_{M\,abs.}$ = Amplification factor for absolute maximum dynamic moment in the bridge based on maximum static moment at mid-span;

and,

$A_{\delta\,1/2}$ = Amplification factor for maximum dynamic deflection at midspan based on maximum static deflection at mid-span.

Some of the results obtained from the analyses of these problems are shown graphically herein in Figures 6 to 11, which are typical of the many that have been prepared. Figures 6 and 7 show, for the unsprung case, the amplification factors for moments at mid-span and $3/4$ point for a particular value of weight parameter, R = 0. 50, and for different values of speed parameter $\alpha$ . In these diagrams, the analytical results are represented by solid curves; points identified by circles represent the corresponding experimental results, the determination of which is described in a later section herein. Figure 8 shows, for the unsprung case, values of amplification factors for maximum absolute dynamic moment as a function of the weight and speed parameters, plotted in the form of a contour map. Figures 9 to 11 show similar diagrams for results obtained for the sprung case with zero initial displacement and bouncing velocity.

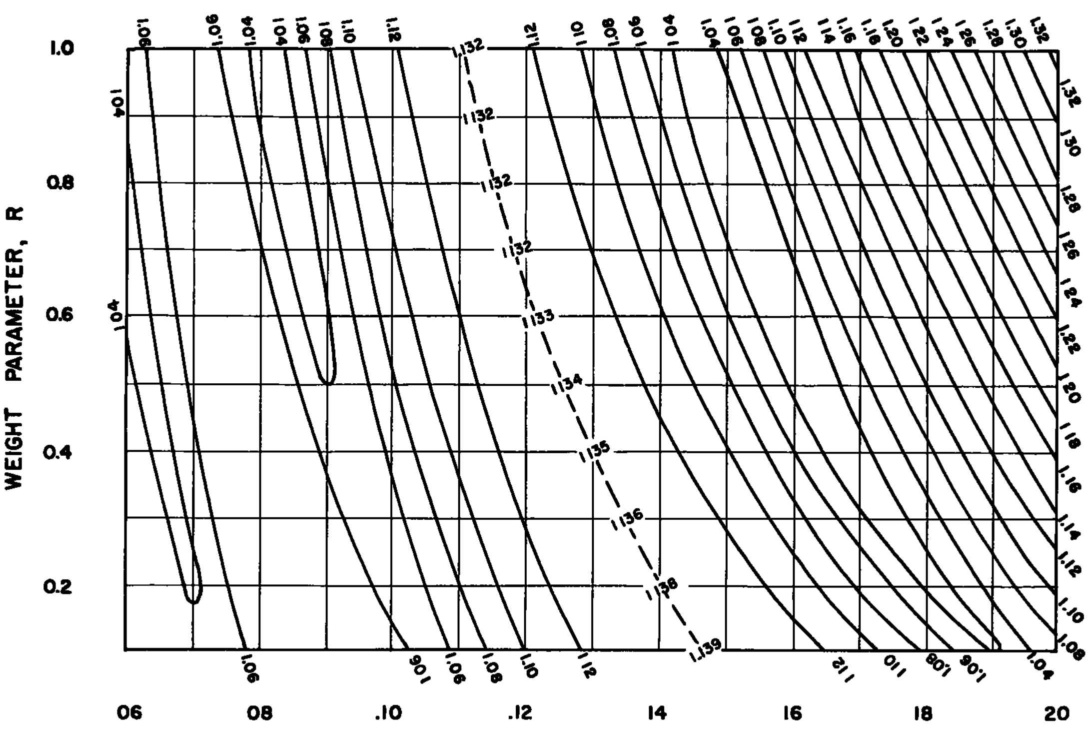


Figure 8. Contour curves of amplification factor for maximum moments, $A_{M_{abs}}$ unsprung vehicle.

The amplification factor for deflection at mid-span was determined also for a variety of conditions. In general, the agreement between the experimentally determined factor and the computed factor for deflection is not nearly as good as for moments. A typical illustration of the results for midspan deflections for a sprung load is shown in Figure 12.

Sprung Mass with Arbitrary Initial Displacement and Velocity. This problem differs from the above two in that here the sprung part of the vehicle has initial deflection and

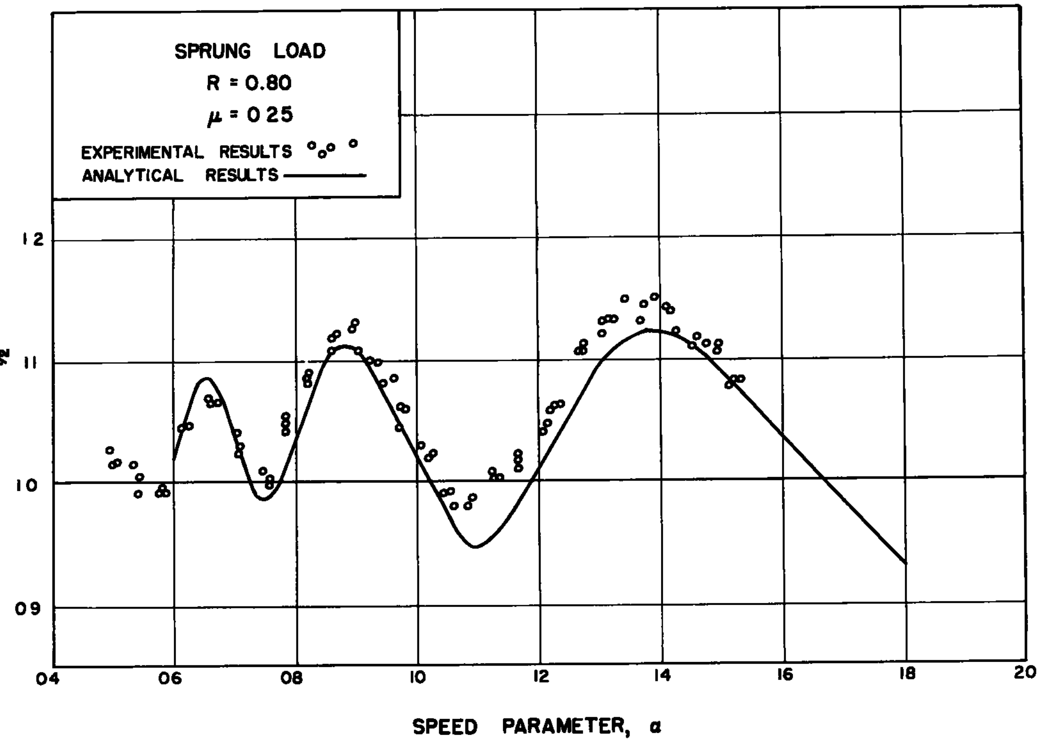


Figure 9. Amplification factor for bending moment at the second quarter point.

bouncing velocity. Since at the moment a vehicle enters the bridge span the sprung part of the vehicle, owing to the presence of pavement joints, wavy road surface in the approach, etc., is seldom stationary at zero displacement, this problem is more realistic than that of the unsprung mass or the sprung mass with zero initial displacement and velocity. One difficulty, however, lies in the selection of appropriate values of the initial deflection and velocity to be prescribed for the sprung mass. In the present study, the problem is so idealized that the initial conditions for the sprung mass are such as to cause very nearly the maximum possible resulting stresses in the bridge. In this way the results obtained constitute the upper limits of impact factors for the worst possible conditions, regardless of what the causes might have been that induced the initial conditions of the sprung mass.

The sprung part of the vehicle could oscillate in various arbitrary ways depending on the conditions of road surface and the speed of the vehicle. In general, its motion involves oscillations of arbitrary amplitude, with varying phase, since the roughness of road surfaces (or other causes) may be imagined to be exerting a series of exciting forces of arbitrary frequency and amplitude. However, in spite of the randomness of these exciting forces, the moving vehicle does possess a certain definite characteristic in its response to the exciting forces; and it is not unreasonable to assume that the motion of the sprung mass is predominantly one in which it vibrates at its own frequency, but with a certain amplitude, which can be determined either from field measurements or from statistical analysis based on pertinent data.

Following the assumption that the sprung mass vibrates at its own frequency with a given amplitude, it is reasonable, in order to obtain the maximum impact stresses in the bridge, to adjust the initial conditions in such a way that the maximum compression in the spring is developed just at the instant that the vehicle reaches a certain section near mid-span, where the dynamic stresses in the bridge due to the weight of the truck alone are also maximum for the whole bridge. Now, the maximum compression in the spring does not develop except with the simultaneous occurrence of a maximum downward deflection and a maximum rebound of the bridge. However, the maximum spring compression does not usually synchronize with the maximum dynamic stress due to the weight of the vehicle alone except for very low speeds or very long spans. This is because the maximum rebound of the bridge generally occurs, for average vehicle speeds and span lengths, when the vehicle has already passed the section near mid-span, where the maximum dynamic stresses due to the weight of the vehicle alone are obtained. To overcome this difficulty in the analyses, the maximum downward deflection of the sprung mass, instead of the maximum compression in the spring, is therefore adopted as a more convenient criterion for synchronization; that is, the initial conditions are adjusted such that the maximum downward deflection of the sprung mass is obtained at the instant that the maximum dynamic stresses due to the weight of the truck alone are obtained. This leads to a slight degree of approximation in the method, which is discussed subsequently.

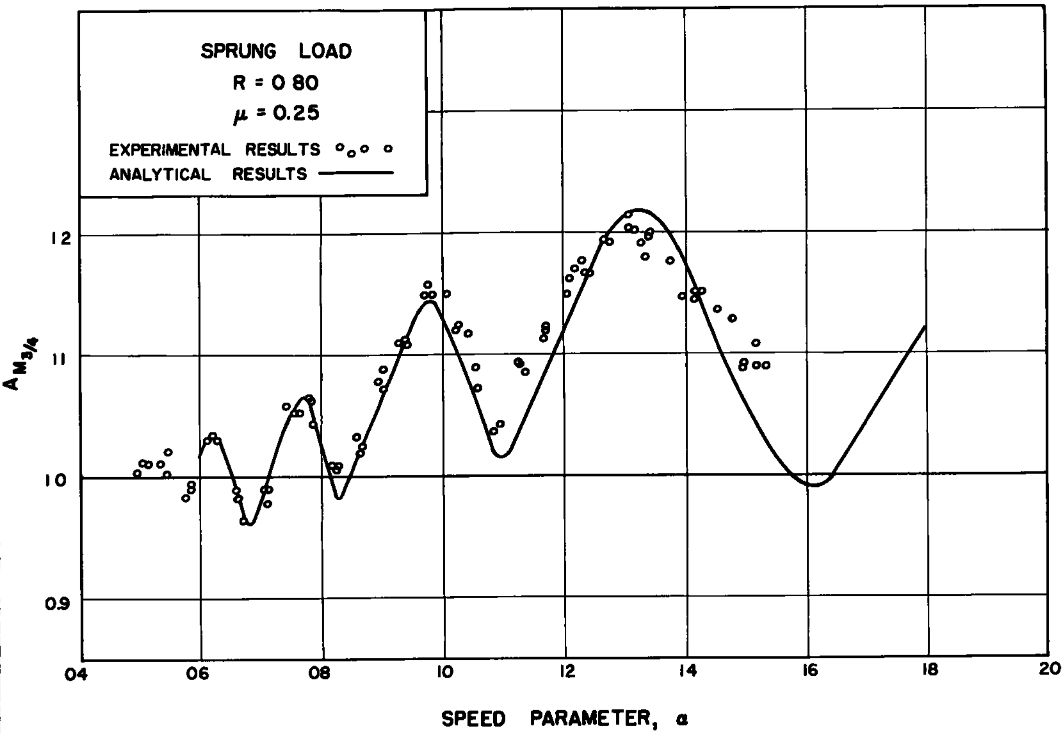


Figure 10. Amplification factor for bending moment at the third quarter point.

The use of the maximum downward deflection of the sprung mass as a criterion for synchronization may be expressed symbolically in the following manner:

The deflection, $y_2$, of the sprung mass at any time t may be represented by

$$y_2 = y_{2_0} \cos pt + \frac{v_{2_0}}{p} \sin pt$$

in which $y_{2_0}$ = initial deflection of the sprung mass,

$v_{2_0}$ = initial velocity of the sprung mass,

$p$ = circular frequency of the sprung mass.

If $A_0$ is the amplitude of oscillation of the sprung mass, then

$$y_{2_0} = A_0 \cos \theta ;$$

$$\frac{v_{2_0}}{p} = A_0 \sin \theta ;$$

and

$$y_2 = A_O (\cos \theta \cos pt + \sin \theta \sin pt),$$

in which $\theta$ = phase angle.

Obviously, $y_2$ will attain a maximum value equal to $A_O$ at time $t_1$ if the phase angle, $\theta$, is set equal to $pt_1$.

The maximum dynamic stresses may then be computed using an iterative procedure. Thus,

1. Assume a value for $t_1$.
2. Using this value of $t_1$, calculate the phase angle, $\theta$, from which the initial displacement and velocity, $y_{2_O}$ and $v_{2_O}$, respectively, of the sprung mass may be found.
3. With these values of $y_{2_O}$ and $v_{2_O}$ as initial conditions for the sprung mass, the vehicle-bridge system is analyzed by solving the differential equations of motion. From this is obtained a derived value of $t_1$ at which time the maximum dynamic moment is supposed to occur.
4. If the derived and the assumed values of $t_1$ do not agree, another trial is made using the derived value from the first cycle as the assumed value for the second cycle. The process is repeated until a good agreement between the assumed and derived values of $t_1$ is reached.
5. Using the value of $t_1$ so found, the dynamic stresses calculated will be a maximum.

Using this procedure, computations for amplification factors for absolute maximum dynamic moment were made for a large number of structures. Figure 13 shows the analytical results obtained for a typical structure, for two values of the initial amplitude of the sprung mass, $A_O$, which are represented in the diagram by the dimensionless quantities, $\bar{A}_O = 1.5$, and $\bar{A}_O = 3.5$. These values of $\bar{A}_O$ correspond roughly to amplitudes of 1 in. and 2 in. for a heavy truck on a 60 ft. span bridge. A larger amplitude corresponds to poorer road surface conditions, and therefore, as may be expected, produces higher dynamic stresses.

From a large number of computations diagrams were prepared, of which Figure 13 is typical. It is found that for a given amplitude the amplification factor for absolute

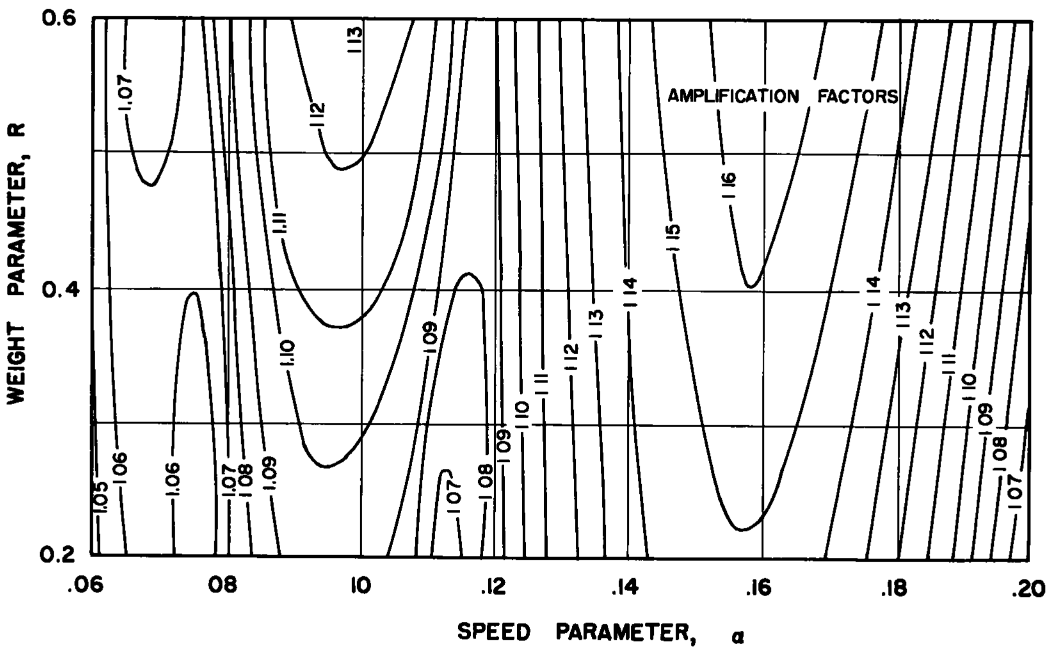


STIFFNESS PARAMETER, $\mu$ = 0 30

Figure 11. Contour curves of amplification factor for absolute maximum moments. Sprung vehicle with zero initial displacement and bouncing velocity.

maximum moment does not vary appreciably with changes in the speed parameter, α. Each of the two curves shown in Figure 13 is seen to consist of several parts; each part corresponds to a certain phase angle, θ. It is possible to have, for a single value of α, two values of amplification factor, one corresponding to one value of phase angle and the other corresponding to another value of phase angle. In that case, the larger of the two amplification factors is plotted as a point on the solid curve.

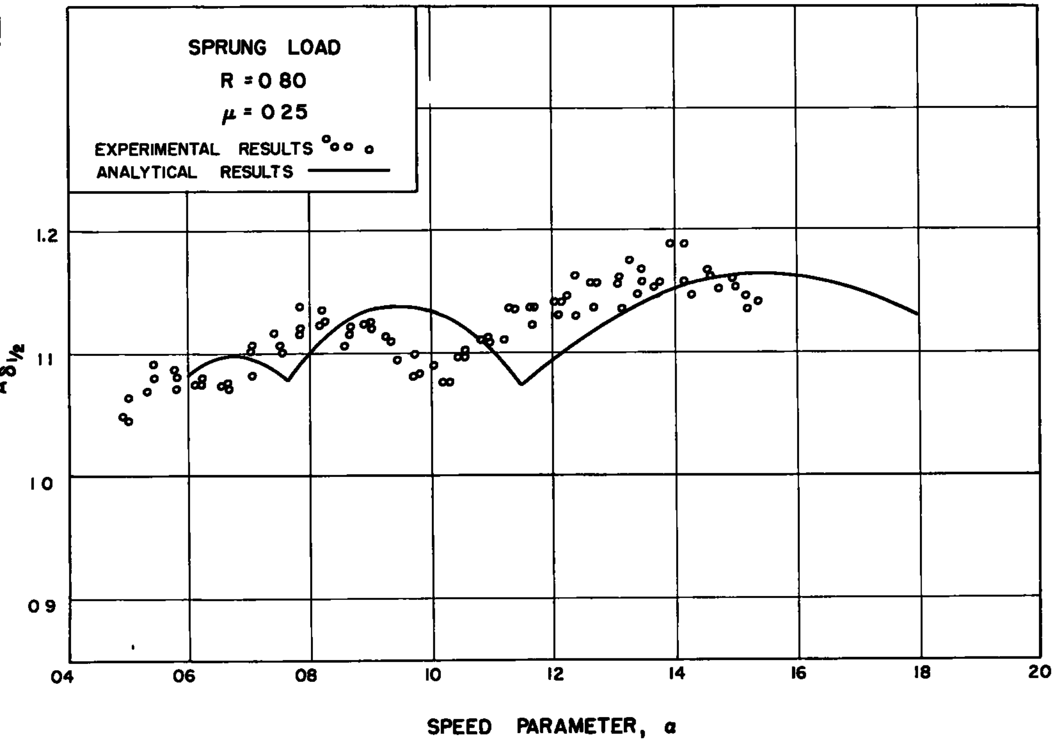


Figure 12. Amplification factor for deflection at the second quarter point.

In the development of the principles underlying this analysis, it was assumed that corresponding to time $t_1$, the phase angle θ may be calculated from the relationship, $\theta = pt_1$. To justify this assumption, a series of computations of maximum impact factors for moment were made using an exact method. In this exact method, a value of θ was first assumed and the maximum dynamic moment calculated. Then another value of θ was assumed differing by a small amount from the previous value of θ, and the corresponding maximum dynamic moment was again calculated. From a number of such calculations, the largest value of the maximum dynamic moment was found. The results of this exact procedure, which is free of the assumption mentioned above, are listed in Table 1, which also contains the corresponding results of the approximate procedure. Referring to Table 1, it is seen that the errors of the approximate method are within one percent. Since the exact method takes about four times as long as the approximate procedure, the simplifying assumption is well justified.

## EXPERIMENTAL INVESTIGATION

### General

The experimental phase of this investigation has been conducted on model structures for the purpose of checking analytical results, and also to provide certain guides for the performance of controlled field tests contemplated for the future. The laboratory experiments have been planned to reproduce as closely as possible, on a scale model, the dynamic effects of the idealized structure considered in the analysis.

TABLE 1

$\bar{A}_0 = 3.5$, $\mu = 0.25$, $R_2/R_1 = 6.05$, $R = 0.80$

| Speed Parameter $\alpha$ | Maximum Amplification Factors for Moment | |
|---|---|---|
| | Approximate Method | Exact Method |
| 0.180 | 1.359 | 1.360 |
| 0.175 | 1.372 | 1.374 |
| 0.170 | 1.381 | 1.385 |
| 0.165 | 1.392 | 1.394 |
| 0.160 | 1.396 | 1.401 |
| 0.155 | 1.395 | 1.404 |
| 0.150 | 1.401 | 1.405 |
| 0.145 | 1.395 | 1.404 |
| 0.140 | 1.395 | 1.399 |
| 0.135 | 1.383 | 1.393 |
| 0.130 | 1.378 | 1.383 |
| 0.125 | 1.360 | 1.371 |
| 0.120 | 1.350 | 1.355 |

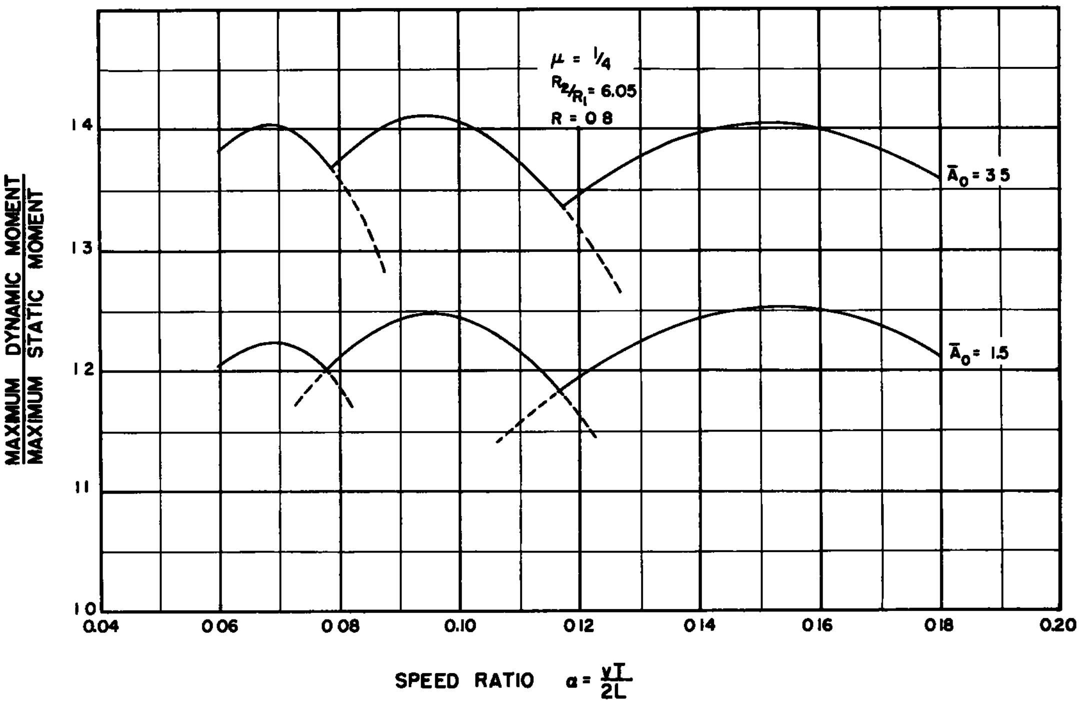


Figure 13. Synchronized amplification factor, $A_{M_{abs}}$, sprung vehicle with arbitrary initial conditions.

A brief description of the test equipment and procedure is given in the following sections. For a fuller and more detailed account of the experimental program, reference is to be made to theses by Milley (5), Boehning (3), and Eichmann (6).

## Description of Apparatus

The test apparatus essentially consists of five parts: the test beam, the load carriage, the launching device, the approach track and the arresting device. Figure 14 shows a general view of the apparatus, and Figure 15 shows close-ups of the main features of the apparatus.

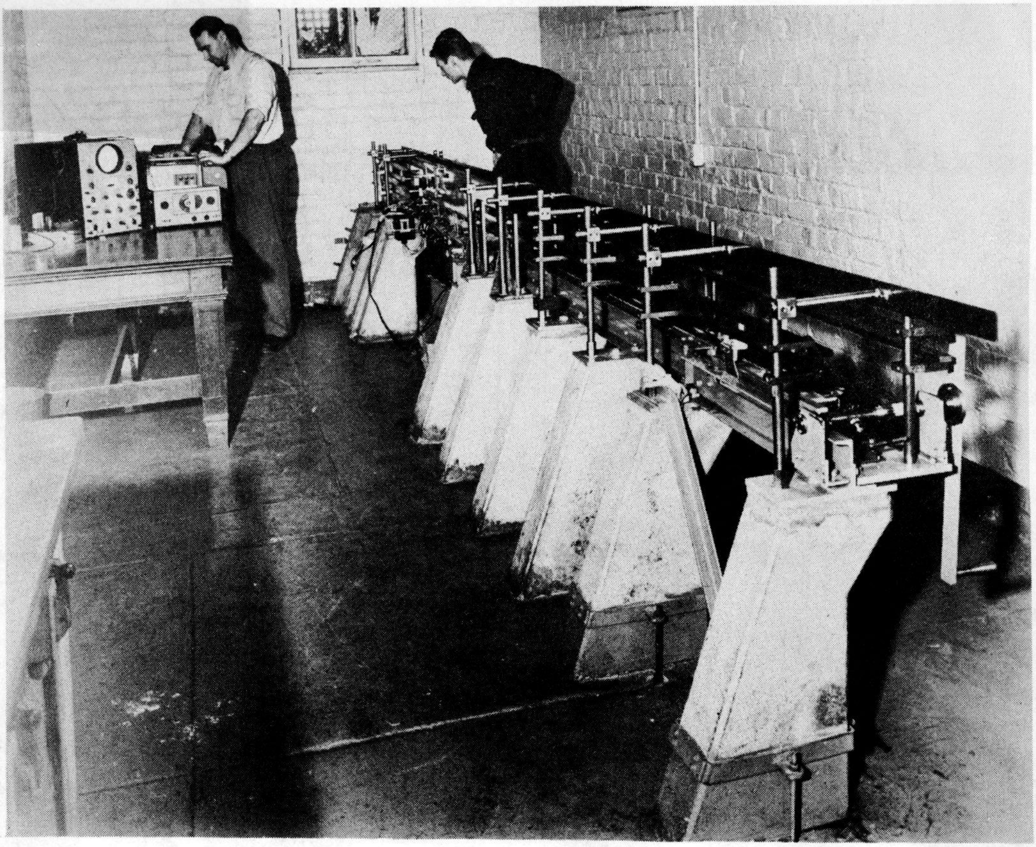

Figure 14. General view of the apparatus.

Test Beam. A schematic drawing of the test beam is shown in Figure 16, in which its dimensions and physical properties are also given. SR-4 strain gages were placed every 6 inches along the 6 foot length of the beam. In addition to these, a set of gages was placed at a point 2¼ inches beyond the mid-span of the beam near where absolute maximum moments are expected to occur. The increase in weight of the beam, due to the addition of the strain gages, was taken into account in subsequent reduction of test data. The natural frequency of the beam with the gages was computed, and later checked by actual measurements. The effect of damping of the beam had been evaluated by a separate test, and it was found that the small amount of damping present may be neglected for all practical purposes.

The gap between the test beam and the approach track was set at a few thousandths of an inch. To reduce the entrance impact, a thin strip of shim stock, filed to a feather edge, was placed across the gap.

Load Carriage. Schematic drawings showing the general dimensions and features of the load carriage are shown in Figures 17 and 18.

Two double elliptical springs were used in the carriage to simulate the effect of vehicle suspension. After they were assembled, they were subjected to load-deflection tests, from which an average spring constant was determined. From this value the natural frequency of the sprung mass was calculated, and it was also checked by actual measurement.

It had previously been found that the natural frequency of the average simply supported I-beam highway bridge, which the model beam represents, is about 6.4 cycles per second. Also, from investigations of commercial trucks, the natural frequency of a heavy truck was found to be about 100 cycles per minute. Thus, the ratio, $\mu$, of the natural frequency of the vehicle to that of the bridge, for the prototype was fixed

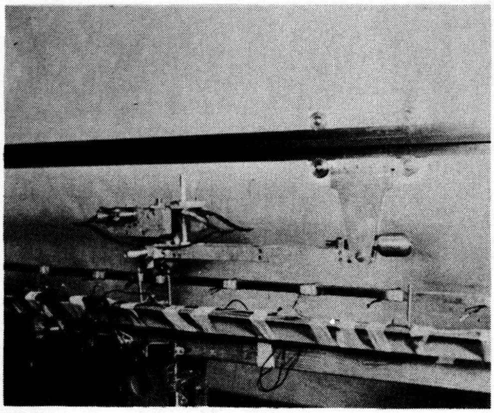

SPRUNG LOAD CARRIAGE

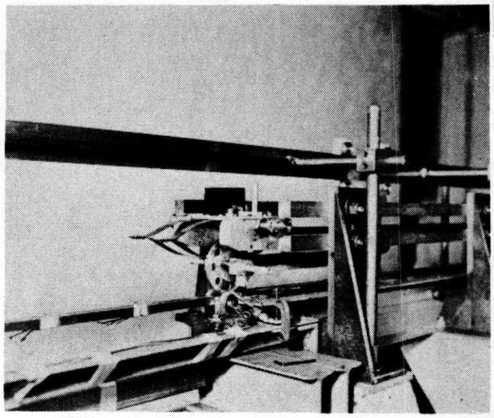

GUIDE TRACKS

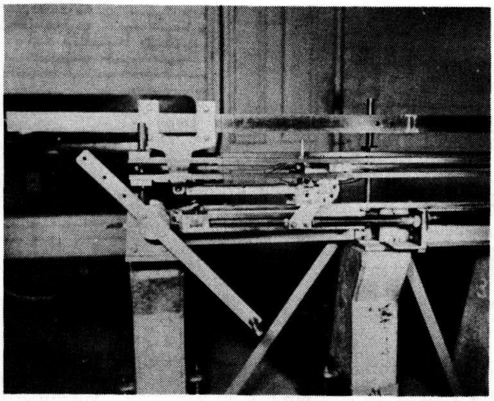

LAUNCHING MECHANISM

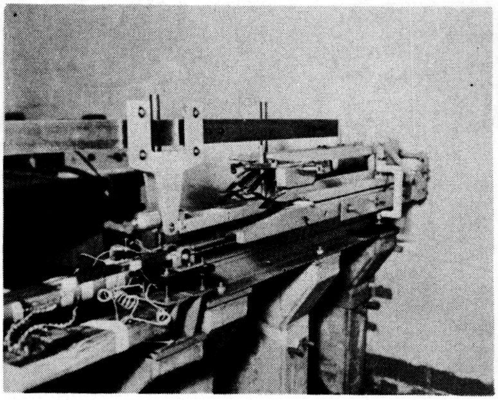

RESTRAINING DEVICE

Figure 15. Details of the apparatus.

at 0.26. In order to have a dynamically similar model, this ratio $\mu$ must be the same for both model and prototype. The value of $\mu$ for the model was found to be 0.25, which was considered sufficiently close to the desired value.

Running directly above and parallel to the test beam was a rigid track over which a four wheel trolley was designed to hook so that the carriage was allowed to pivot freely about the same point at which the rear axle was located. The dynamical balance of the carriage was maintained by means of the counterweight at the rear of the carriage.

Launching Device. A tension spring launching mechanism was used. This was adopted in preference to allowing the carriage to run down an inclined plane because of the greater speed that could be developed in the carriage before crossing the test beam. The launching device or catapult consisted of three tension springs connected to a rachet bar. Two uprights attached to the rachet engaged the front axle of the carriage to transmit to the carriage the energy stored in the stretched springs. Brackets were bolted to the uprights to engage the sprung part of the carriage; this served to distribute the shock more evenly to the parts of the carriage. The rachet bar was pulled back by means of a gear and crank arrangement. The gear was free to slide on a keyed shaft and could be pushed aside once the bar had been pulled back the desired distance and locked in place by the release button. This crank arrangement greatly reduced the effort required to pull back the rachet to a 200 lb. spring tension and made it much easier to engage the desired notches on the rachet. The rachet notches were numbered and by calibrating the device for various carriage weights, the speed of the carriage was known in advance very closely.

The stability of the launching mechanism was assured by bolting its concrete supporting piers to the floor. Under this arrangement vibrations were transmitted through the floor to the test beam. To remedy the situation, an air brake was installed to cushion the launching springs, thereby relieving the hammer blow effect of the springs.

Approach Track. After the carriage was given its initial velocity by the launching springs, it was guided onto the test beam by means of a horizontal approach track, placed directly in line with the beam. A single length of smooth steel was supported on the top flange of a built-up I beam which in turn was bolted to five concrete pedestals. The carriage wheel ran on the track and was kept in a straight line by means of two brass strips with sloping sides forming a groove the same shape as the running wheel.

A pair of guide tracks, one above the other, was mounted on each side of the approach track. A bar was attached to each side of the sprung weight and bearings were mounted at the ends of the bars. The resulting trolleys then ran between the external rigid guide tracks and served to keep the weight from bouncing until it reached the beam.

Arresting Device. After the carriage had crossed the beam, it was stopped by the frictional forces developed between strips of wood 3 feet in length which caught the axles of the carriage. Two additional wooden stops were used to retard the motion of the sprung mass. Two quick-action clamps were put into the axle stops to ease removal of the carriage from the arresting device.

## Testing Program

The first part of the test program was concerned with the instantaneous stress distribution for several different values of speed parameter, $\alpha$ , both for the sprung and unsprung cases. It was this series of tests that afforded the basis for a simplified approximation introduced in the analytical study, as mentioned earlier.

The second part of the program determined the amplification factors for bending

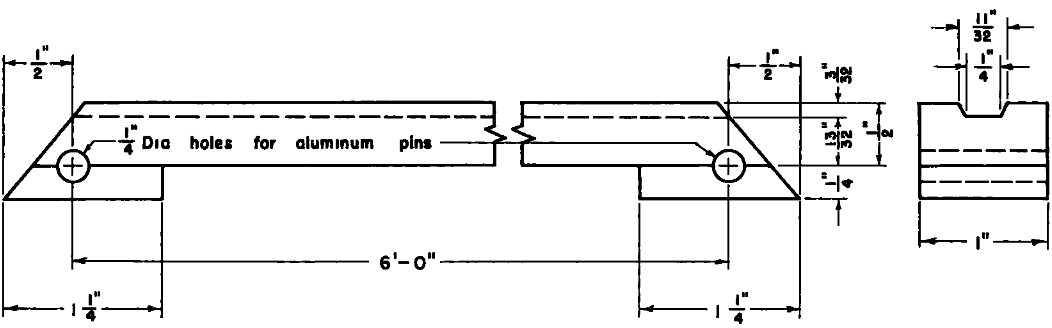


TEST BEAM

| Span | Weight | Calculated Fundamental Frequency | Moment of Inertia | E |
|---|---|---|---|---|
| 6.00 ft. | 9.59 lb.+ | 8.56 cycles per second | .0091 in.$^4$ | $30.8 \times 10^6$ psi |

+ Excluding weight of end plates and gages

TEST BEAM DETAILS

Figure 16.

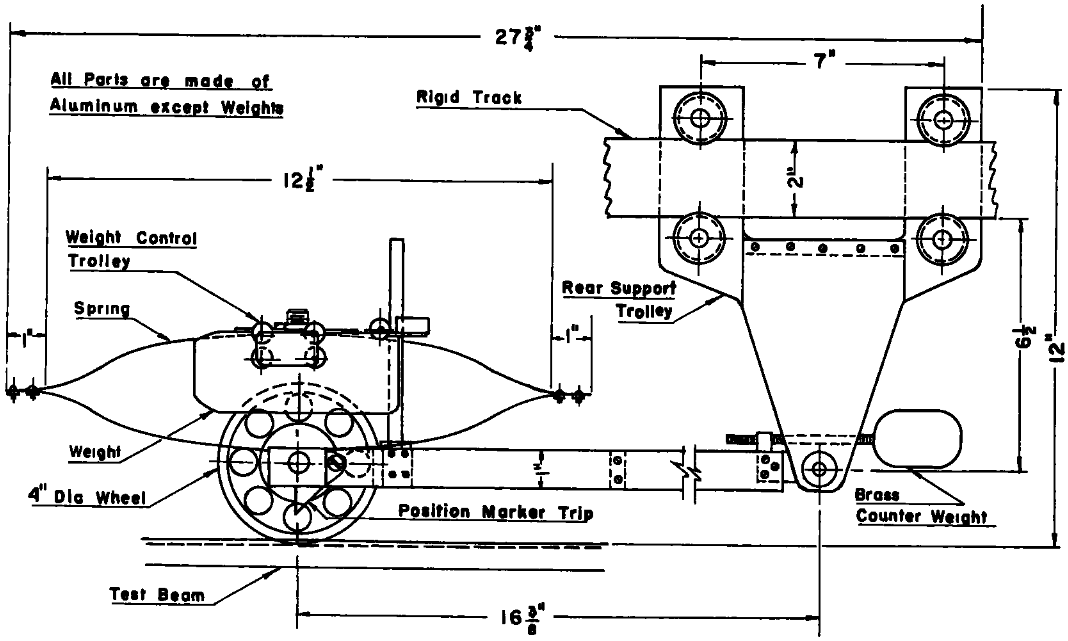


Figure 17. Load carriage, side view.

moments and deflection due to a single unsprung load traversing the beam at constant velocity. Only one set of values of the weight parameter, R, and stiffness parameter, $\mu$, was investigated over a range of velocities corresponding to values of the speed parameter, $\alpha$, from 0.05 to 0.14. Three to four test runs were made at each velocity to check the reproducibility of results. Dynamic bending moments were recorded at the second and third quarter points and at a point close to the second quarter point. Dynamic deflections were recorded at the mid-span only.

Another complete set of tests similar to those just mentioned was run for a sprung mass traversing the beam at constant velocity and having zero initial displacement and bouncing velocity at the moment it entered the span.

For the case of a sprung mass having initially arbitrary displacement and velocity, a series of tests was started and is now in progress. In each of the several groups of tests in this series a single value of the speed of the carriage is used, while the initial conditions of the sprung mass are varied by varying the position of release of the carriage. Strains are measured at a sufficient number of points for the determination of the maximum dynamic stress in any given case. Deflections are recorded at the mid-span of the beam only.

## Testing Procedure

At the beginning of each day's testing a determination of the natural frequency of the beam was made. The daily determinations were believed essential to detect any changes that might have occurred in the test apparatus. Following the determination of the natural frequency, two determinations were made of the maximum static bending moment and deflection for each active gage. This was done first by placing the load carriage successively over each active gage and making a record of the strains and moments. A "crawl" static run was then made by pushing the carriage across the beam slowly enough so as not to create a dynamic effect. The results of these two tests were averaged. Static determinations were also made after each set of 15 runs.

To check reproducibility of results, three runs were made at each rachet reading. This resulted in three amplification determinations for a small range of $\alpha$. Due to limitations of the launching mechanism, the velocities would not always be reproduced exactly. However, since the velocity was determined separately for each run and the variation in velocity for each set of rachet readings was small, the result was a group of three points representing essentially the same velocity.

Results of Tests

Typical results of tests have been shown in Figures 6, 7, 9, 10, and 12 for both the unsprung mass and the sprung mass starting from rest. In these figures the test results are represented by points identified by circles. The most striking feature of the test results is the close agreement with the predictions of the calculations made by the simplified theoretical procedure described herein. It should be emphasized, however, that it was necessary to conduct the tests with great care in order to eliminate erratic variations in the results. The smoothness of the experimental data was obtained only after all extraneous variables were controlled. Minor roughness in the test track and minor velocity variations, before precise procedures were developed, contributed to large variations in pilot tests. These variations have been successfully eliminated, as shown by the data presented.

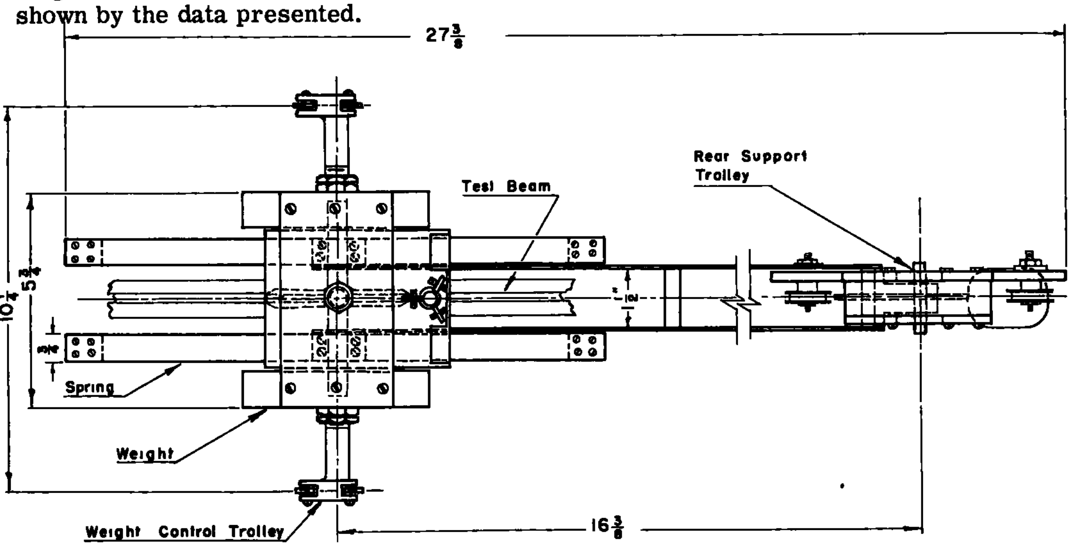


Figure 18. Load carriage, top view.

## DISCUSSION OF RESULTS

The results which have been reported only in summary form in this paper are in themselves sufficient, however, to substantiate certain general conclusions. These conclusions are supported by more complete data which have been obtained on the program, but which are not presented herein because of limitations of space. It is clear from the work which has been done that the analytical procedure described leads to results which are quite reasonable for the bending moments in the structure. The deflections are not predicted quite so accurately by the theory, but the deflections are not nearly as important in the design of the structure as the stresses or bending moments.

The amplification factor or impact effect for maximum moment for an unsprung vehicle is relatively small. The impact effect is less than 30 percent for values of the speed parameter less than about 0.20 and for values of the weight parameter, R, less than about 1.0. This range includes most of the practical ranges of parameters for highway bridges. Moreover, the amplification factor is considerably lower than the maximum value as the weight parameter or the speed parameter decreases below the maximum values mentioned.

It is also clear that there is a good deal of variation in the amplification factor with variation in the speed parameter. The curves of amplification factor plotted against speed parameter, shown in Figures 6 and 7, are typical of the oscillatory nature of the amplification factor as a function of speed.

Similar conclusions can be drawn with regard to the effect of a sprung load which is not in oscillation at the time the load enters the bridge. As a matter of fact, the amplification factors are not greatly different from those for an unsprung load under these conditions, and the oscillatory nature of variation of the amplification factor with speed is also evident for a sprung mass which is not bouncing when it enters the bridge.

Because most highway vehicles have the major part of their mass supported on springs of varying characteristics, and because unevenness in the roadway pavement before the vehicle reaches the bridge, or abrupt changes in elevation or grade at the entrance to the bridge, generally always cause some oscillation of the mass supported on the springs of the vehicle, in most practical cases there is a substantial degree of bouncing motion of the vehicle as it passes over the bridge. Even in those cases where this bouncing motion is not evident to begin with, it can be generated during the passage of the vehicle over the bridge. Because the bouncing motion can produce relatively large stresses compared with those produced by a smoothly rolling load, it is desirable to take into account this aspect of the forces producing impact. The results obtained, taking into account the amplification factor for a sprung vehicle with arbitrary initial conditions of motion, are typified by Figure 13. It is immediately evident from a study of this figure that the maximum amplification or the impact effect is much more nearly constant with variation in speed for this condition than it is for the case of an unsprung mass or a sprung load starting from rest. Moreover, the impact factors obtained are considerably larger throughout the range of speeds and mass ratios than for the other cases. In the example cited, for a typical set of parameters, as described in Figure 13, with amplitude of oscillatory bouncing-motion of the sprung mass of the truck amounting to about 1 inch, the impact factor is of the order of 0.20 to 0.25, whereas if the bouncing amplitude is increased to 2 inches the impact varies between 0.35 and 0.4[illegible]

It must be recalled, in this discussion, that these are the maximum values of impact factors for the various conditions which might occur. The curves shown in Figure 13 are envelopes or upper limits to all of the possible impact factors except those which occur due to local irregularities in the roadway on the bridge itself, or to other causes not considered in this analysis. Consequently, the impact factors corresponding to the conditions of zero bouncing velocity when the vehicle enters the bridge are included in the results, of which the values in Figure 13 are upper bounds.

One should consider the significance of these values in terms of the probability of occurrence of the phenomena causing impact. It seems likely that a truck or other vehicle can be oscillating in such a way that it is bouncing with an amplitude equal to the maximum permissible excursion at some time or other during its passage over the bridge. Consequently, provision must be made in the design for the upper limit or envelope curves shown in Figure 13, although this provision need not necessarily be made at ordinary working stresses. However, it is considered to be a much more satisfactory basis for design to use the values resulting from studies such as that reported in Figure 13 rather than to use the data corresponding to Figures 8 and 11.

Probability considerations enter also in multiple lane bridges because of the fact that the maximum stresses arise from trucks in adjacent lanes, and the maximum impact factors would involve trucks moving in such a way as to produce maximum bouncing effects simultaneously in order for the maximum amplitude of vibration to be reached in general.

The studies reported herein do not take into account the possible motion of the bridge prior to the time that a vehicle enters it, arising from other disturbances or from the passage of previous vehicles. Such oscillations can cause an increase even in the values reported in Figure 13. However, in general, the damping of the bridge itself, plus the damping effect of the vehicle traversing the bridge to the center may make this phenomenon of only minor importance compared to the major influence of the bouncing effect of the mass of an individual vehicle. Further studies will be made to throw additional light on this point.

The influence of local roughness of the bridge pavement itself can probably be taken into account by consideration only of the motion of the bouncing mass of the vehicle traveling over a relatively smooth pavement, since these phenomena can be related in terms of the maximum stresses each produces. Further studies of these variables will be undertaken.

Additional and relatively complete studies of the envelope of amplification factors for a sprung vehicle with arbitrary initial conditions are now being made. When these are available it may be possible to develop simple empirical relations which can be used for the determination of impact factors for the design of highway bridges.

Further studies which are underway in the research program at the University of Illinois include the transverse distribution of loading to I-beam bridges from rolling loads in various lanes, and the planning of field test programs for verification of the results of the analysis and laboratory experimental programs.

The use of the high speed digital computer at the University of Illinois has made possible studies which would otherwise be of insuperable difficulty. It is believed that the carefully made laboratory experiments indicate that the assumptions upon which the digital computation is based are valid for the determination of the major effects of impact at least on simple span highway bridges.

## ACKNOWLEDGMENTS

The research reported in this paper was carried on as a cooperative project in the Engineering Experiment Station of the University of Illinois under the sponsorship of the Illinois Division of Highways and the Department of Commerce, Bureau of Public Roads. The work was conducted in the Structural Research Laboratory of the Civil Engineering Department under the general direction of N. M. Newmark. L. E. Goodman was in immediate charge of the program on highway bridge research from its inception to March, 1954, and was responsible for the development of the experimental model program and the general concepts of the analytical work recorded herein. The program on highway bridge impact is now under the immediate supervision of T. Y. Chen. The preparation of the problem for solution on the ILLIAC, and the development of procedures for use of the digital computer on this program were the responsibility of T. P. Tung.

The authors wish to acknowledge the help of a number of their colleagues in the conduct of this program. Particular thanks are due to Dr. A. S. Veletsos and Dr. C. P. Siess, who have been associated in various ways with the work of the Cooperative Highway Research Program at the University of Illinois.

Special acknowledgment is due also to V. J. McDonald, Research Assistant Professor of Civil Engineering, who was responsible for the instrumentation and the recording of the data on the model test beam.

Finally, acknowledgment is due to the graduate students who have worked on this program and have reported the results of their research in masters' theses, parts of which have been used freely in the preparation of this paper. In addition to those mentioned by name in the paper and in the bibliography, acknowledgment is due also to J. E. Taylor for his part in the experimental work.

## *References*

1. Inglis, E. E., "A Mathematical Treatise on Vibrations in Railway Bridges," Cambridge University Press, Teddington, 1934.

2. Timoshenko, S. P. "Vibration Problems in Engineering," 2nd ed., D. van Nostrand Co., New York, 1937, pp. 352-356.

3. Boehning, R. H., "Single and Tandem Axle Dynamic Effects on a Highway Bridge Model," M. S. thesis submitted to the Graduate College, University of Illinois, June 1953.

4. Hillerborg, A., "Dynamic Influences of Smoothly Running Loads on Simply-Supported Girders," Institution of Structural Engineering and Bridge Building of the Royal Institute of Technology, Stockholm, 1951.

5. Milley, W. H., "Experimental Studies of Dynamic Effects of Smoothly Rolling Loads on Simply-Supported Beams", M. S. thesis submitted to the Graduate College,

University of Illinois, June 1952.
6. Eichmann, E. S., "Influence of Vehicle Suspensions on Highway Bridge Impact," M. S. thesis submitted to the Graduate College, University of Illinois, June 1954.